Monthly Notices
of the
ROYAL ASTRONOMICAL SOCIETY

Mon. Not. R. Astron. Soc. **407,** 2157–2165 (2010) doi:10.1111/j.1365-2966.2010.17075.x

A search for interstellar anthracene towards the Perseus anomalous microwave emission region

S. Iglesias-Groth,[1,2★] A. Manchado,[1,2,3] R. Rebolo,[1,2,3] J. I. González Hernández,[1,2,4] D. A. García-Hernández[1,2] and D. L. Lambert[5]

[1] *Instituto de Astrofisíca de Canarias, 38200 La Laguna, Tenerife, Canary Islands, Spain*
[2] *Universidad de La Laguna, E-38205 La Laguna, Tenerife, Spain*
[3] *Consejo Superior de Investigaciones Científicas, Spain*
[4] *Dpto. de Astrofísica y Ciencias de la Atmósfera, Facultad de Ciencias Físicas, Universidad Complutense de Madrid, E-28040 Madrid, Spain*
[5] *The W.J. McDonald Observatory, University of Texas, Austin, TX 78712-1083, USA*

Accepted 2010 May 24. Received 2010 May 21; in original form 2010 March 3

ABSTRACT

We report the discovery of a new broad interstellar (or circumstellar) band at 7088.8 ± 2.0 Å coincident to within the measurement uncertainties with the strongest band of the anthracene cation ($C_{14}H_{10}^{+}$) as measured in gas-phase laboratory spectroscopy at low temperatures. The band is detected in the line of sight of star Cernis 52, a likely member of the very young star cluster IC 348, and is probably associated with cold absorbing material in an intervening molecular cloud of the Perseus star-forming region where various experiments have recently detected anomalous microwave emission. From the measured intensity and available oscillator strength we find a column density of $N_{an^+} = 1.1(\pm 0.4) \times 10^{13}\,cm^{-2}$ implying that ∼0.008 per cent of the carbon in the cloud could be in the form of $C_{14}H_{10}^{+}$. A similar abundance has been recently claimed for the naphthalene cation in this cloud. This is the first location outside the Solar system where specific polycyclic aromatic hydrocarbons (PAHs) are identified. We report observations of interstellar lines of CH and CH^{+} that support a rather high column density for these species and for molecular hydrogen. The strength ratio of the two prominent diffuse interstellar bands at 5780 and 5797 Å suggests the presence of a 'zeta'-type cloud in the line of sight (consistent with steep far-ultraviolet extinction and high molecular content). The presence of PAH cations and other related hydrogenated carbon molecules which are likely to occur in this type of clouds reinforces the suggestion that electric dipole radiation from fast-spinning PAHs is responsible of the anomalous microwave emission detected towards Perseus.

Key words: ISM: abundances – ISM: lines and bands – ISM: molecules.

1 INTRODUCTION

Several regions in the Perseus molecular complex display a strong continuum microwave emission in the frequency range 10–60 GHz that is correlated with dust thermal emission (Watson et al. 2005; Tibbs et al. 2010). The spectral dependence of this emission cannot be explained by synchrotron, free–free or thermal dust radiation processes, and represents one of the best known examples of the so-called anomalous microwave emission (Kogut et al. 1996; Leitch et al. 1997; de Oliveira-Costa et al. 1999, 2002). This kind of microwave emission is also detected in other molecular clouds (Casassus et al. 2006), and there is increasing statistical evidence supporting its existence at high Galactic latitudes (Hildebrandt et al. 2007). Draine & Lazarian (1998) suggested a possible explanation for this emission based on electric dipole radiation from rapidly spinning carbon based molecules (see also Iglesias-Groth 2005, 2006). Polycyclic aromatic hydrocarbons (PAHs) proposed as the sources of interstellar mid-infrared emission (Allamandola, Tielens & Barker 1989; Puget & Léger 1989) and diffuse interstellar bands (Allamandola et al. 1989; Puget & Léger 1989) are also potential carriers for the anomalous microwave emission. It is likely that anomalous microwave emission surveys reveal interstellar regions of enhanced PAH abundance and therefore further studies of these regions may facilitate the identification of individual PAHs. Recent progress in the laboratory measurements of optical and near-infrared bands of the most simple PAHs and their cations under conditions resembling the interstellar medium is a key step to this aim (e.g. Salama 2008).

★E-mail: sigroth@iac.es

Here, we report results on a search for interstellar bands in the line of sight of the maximum anomalous microwave emission detected towards the Perseus clouds (Tibbs et al. 2010). We obtained high-resolution optical spectroscopy of Cernis 52 (BD+31° 640), a reddened star [$E(B-V) = 0.9$; Cernis 1993] located in this line of sight at a distance of 240 pc where most of the dust extinction is in the Perseus OB2 dark cloud complex. This is the brightest hot star that we could identify as a suitable background object to study the interstellar absorptions in the intervening cloud. Very recently, evidence was reported for absorption bands of the naphthalene cation $C_{10}H_8^+$ in the line of sight of this star (Iglesias-Groth et al. 2008). A detailed chemical composition study of this star has been published by González Hernández et al. (2009). We report now evidence in this line of sight for the next PAH in terms of complexity, the anthracene molecule which is composed of three aromatic rings. Laboratory spectroscopy of the anthracene cation ($C_{14}H_{10}^+$) obtained using supersonic jet-discharge cavity ring-down spectroscopy (Sukhorukov et al. 2004) to resemble the conditions of the interstellar medium has provided an accurate measurement of the strongest vibronic band for the $D_2 \leftarrow D_0$ system of this molecule. The laboratory band is measured at the wavelength of 7085.7 ± 1.3 Å (in standard air) with a full width at half-maximum (FWHM) of ∼47 Å. We obtained spectra of Cernis 52 and found a new broad interstellar feature with wavelength and width consistent with the measurements for the strongest optical transition of the anthracene cation. We also present new measurements of interstellar absorption lines of CH and CH^+ and of the most prominent diffuse interstellar bands, providing insight on the physical and chemical processes in the intervening medium.

2 OBSERVATIONS

We report spectroscopy of Cernis 52 obtained with (a) the ISIS spectrograph (grating R1200B and R1200R for the blue and red arms, respectively) at the 4.2-m William Herschel Telescope (WHT), at the Roque de los Muchachos Observatory (La Palma, Spain) on 2007 and 2008 December; (b) the High-Resolution Spectrograph (HRS) of the 9.2-m Hobby–Eberly Telescope at the McDonald Observatory (Texas, USA) on several nights during 2008.

Comparison stars were observed with the same instruments on the same nights for correction of telluric lines and control of the instrumental response. All the spectra were reduced using IRAF, wavelength calibrated with less than 20 mÅ rms error and individual spectra were co-added after correction for telluric lines. The adopted slit width for ISIS (1.00 arcsec) led to a spectral resolution of 0.8 and 0.6 Å for the blue and red arms of ISIS, respectively. The fibre used to feed HRS led to a spectral resolution of 025 Å in the spectral regions of interest. The zero-point of the adopted wavelength scale was set by assigning the laboratory wavelength to the K I 7698.974 Å interstellar absorption line. We plot in Fig. 1 one of the spectra of Cernis 52 obtained at the WHT. This spectrum was extracted using the IRAF routine 'APSUM' after bias and flat-field correction of the original spectral image. We show the spectrum with no normalization applied, only division by a constant, and also show the result of normalization using a low-order polynomial fit. We note the smooth behaviour of the continuum and the presence of several broad absorption features and narrow telluric lines. The continuum correction does not affect these features. The WHT spectra help to define the continuum regions used for normalization of the echelle spectra obtained at the HET.

The Cernis 52 spectra from both telescopes were corrected for telluric line contamination and possible instrumental effects dividing each individual spectrum (15 were recorded at the HET) by the almost featureless spectrum of a much brighter, hot and fast-rotating star in a nearby line of sight observed with the same instrument configuration. After this correction, individual spectra were normalized using a polynomial fit to the continuum regions and then combined to improve signal-to-noise ratio (S/N). The final WHT and HET spectra are plotted at the top of Fig. 2 (red and blue solid lines,

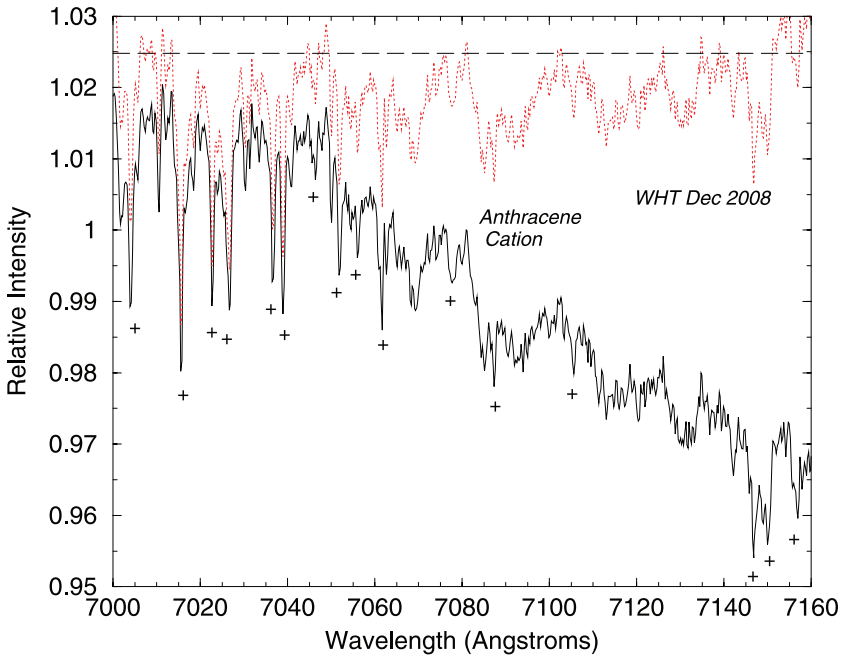

Figure 1. Spectrum of Cernis 52 obtained at the WHT with ISIS (grating R1200R) on 2008 December before (solid black line) and after (red dotted line) normalization of the continuum. The strongest telluric lines are marked. The dashed line indicates the location of the continuum.

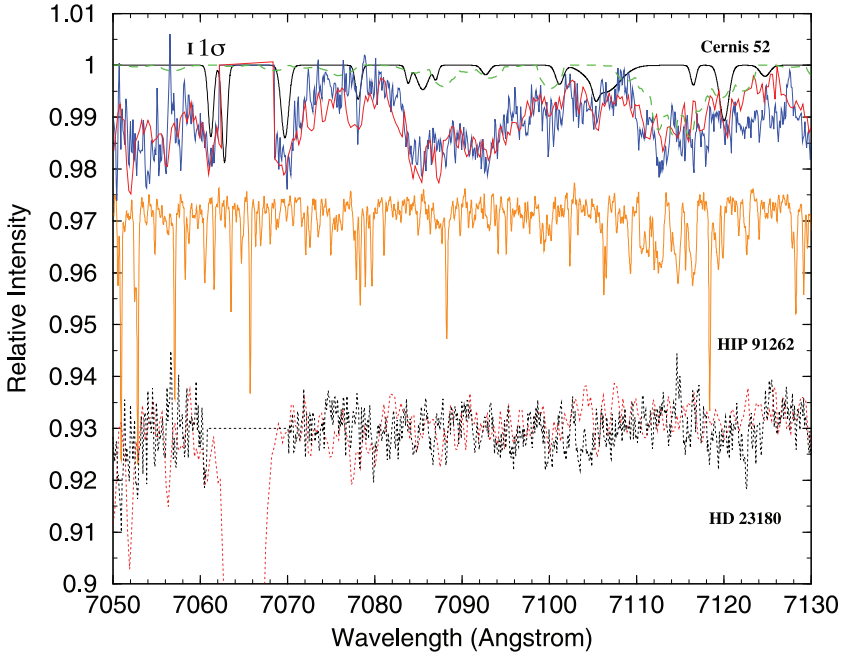

Figure 2. Top: final spectra of Cernis 52 (WHT: red line; HET: blue line) showing two independent detections of the new 7088.8 Å band ascribed to the anthracene cation. 1σ error bars are indicated. Both spectra have been corrected for telluric lines using rapidly rotating hot stars observed with the same instrumental configuration. Telluric absorptions were divided out except in the range 7060–7070 Å where an He line present (see the spectrum at the bottom) prevents this correction. The uncorrected spectral region has been set at unity. A photospheric spectrum (dashed green line) computed for the stellar parameters of Cernis 52 (see the text for details) and a DIB synthetic spectrum (solid thin black line) based on data from Hobbs et al. (2008, 2009) are overplotted. Middle: spectrum of the comparison AO-type star HIP 91262 (thin red line) from Allende-Prieto et al. (2004). The narrow absorptions indicate the location of telluric lines which were largely corrected for Cernis 52. Bottom: spectra of the reference hot star HD 23180 (WHT: red line; HET: dotted black line) observed with the same instrumentation than Cernis 52. The HET spectrum was divided by the same fast rotator used for Cernis 52. No division was applied to the WHT data in order to show the He 7065 Å absorption and the strength of telluric lines.

respectively). We remark the good agreement between the WHT and HET spectra (both with S/N $\geq$ 300 pixel^{-1}). These two spectra contain stellar photospheric features as well as bands associated with circumstellar or diffuse interstellar material in the line of sight (Iglesias-Groth et al. 2008; González Hernández et al. 2009). Cernis 52 is embedded in a cloud responsible for significant visible extinction ($A_V \sim 3$), and the presence of absorption bands caused by the intervening interstellar material was therefore expected.

3 RESULTS AND DISCUSSION

In both spectra of Cernis 52 plotted in Fig. 2, we note the presence of a broad absorption in the range 7075–7105 Å. This is the range where absorption from the most intense band of the anthracene cation is expected. As we can see there is no similar absorption feature in the spectrum of the nearby hot star HD 23180 (Cernis 67, also known as o Per) plotted at the bottom. This star is located in Perseus close but outside the region of anomalous microwave emission. It was observed with the same instruments and with similar S/N to Cernis 52 at both telescopes. The HD 23180 and the Cernis 52 spectra were divided by the same spectra of fast-rotating stars to correct for telluric absorptions. The rather flat spectra of HD 23180 indicate that the broad absorption feature in the range 7075–7105 Å found in Cernis 52 is not an artefact introduced by the instrument or the reduction procedure. In Fig. 2, we can see the absence of broad absorptions in the spectrum of the A0V star HIP 91262 taken from the data base by Allende-Prieto et al. (2004). The very narrow absorptions are telluric lines. The most significant photospheric absorption in this star is located in the range 7110–7120 Å where we also see absorption in the spectrum of Cernis 52. This is mostly caused by photospheric CI lines.

In what follows we show in more detail that the broad absorption in the range 7075–7105 Å does not originate in the photosphere of Cernis 52. We computed a synthetic spectrum of Cernis 52 using the atmospheric parameters and metallicity derived for this star by González Hernández et al. (2009). We adopted $T_{\rm eff} = 8350$ K, $\log(\mathrm{g\,cm^{-1}\,s^{-2}}) = 4.2$ and [Fe/H] $= -0.01$. The synthetic spectrum was broadened to match the rotational velocity of the star ($v \sin i = 65\ \mathrm{km\,s^{-1}}$). In González Hernández et al., evidence is reported for veiling of the photosphericspectrum; they find that almost half of the total observed flux at 5180 Å is contributed by the photosphere of Cernis 52. We also find that the synthetic spectrum has to be veiled by an amount comparable to the flux in the continuum in order to match the photospheric features in the 7110–7120 Å region. The veiled synthetic spectrum is plotted at the top of Fig. 2 (dashed green line) where we can see there are only very weak photospheric absorptions in the range 7050–7110 Å which cannot explain the broad feature detected in the spectrum.

As an additional check, we compared our synthetic spectra with stellar spectra available in the compilation by Allende-Prieto et al. (2004) and verified that the photospheric features of stars with spectral type similar to Cernis 52 were properly reproduced. To illustrate this, we plot in Fig. 3 the synthetic spectrum computed for Cernis 52 and compare it with the spectrum of the A3 V star HIP 57632 (corrected for telluric lines) and broadened to the rotational velocity of Cernis 52. The reference star shows no significant photospheric absorptions in the 7075–7105 Å range. The main photospheric absorption is the CI blend at 7110–7120 Å which is reasonably well

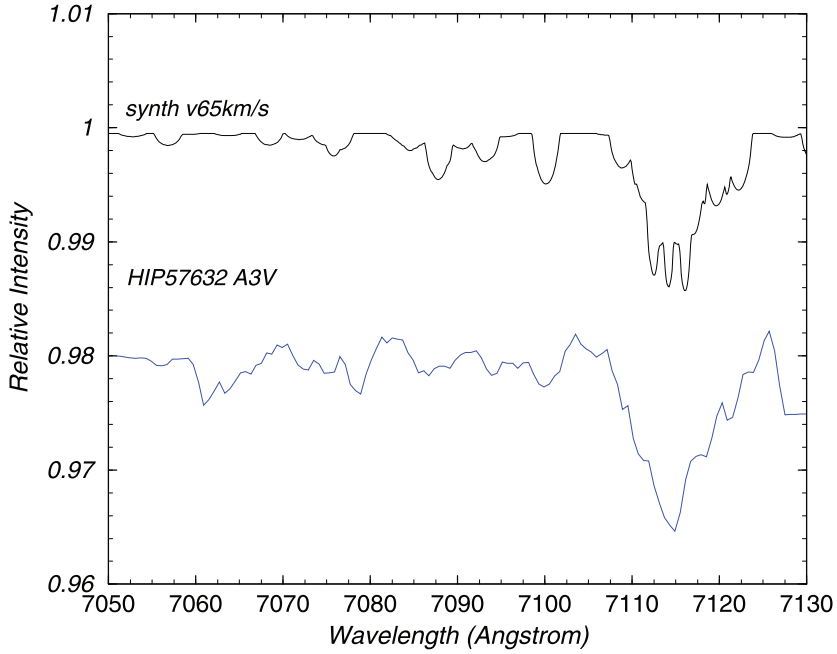

Figure 3. Top: synthetic spectrum computed for the stellar parameters of Cernis 52. Bottom: spectrum of the star HIP 57632 (A3 V) from Allende-Prieto et al. (2004) boxcar smoothed to match the rotational velocity of Cernis 52. Telluric lines are corrected.

reproduced in the computed spectrum. We trust our spectral synthesis can reproduce the observed features in the spectra of stars similar to Cernis 52 and therefore conclude that photospheric lines cannot explain the broad absorption detected in the range 7075–7105 Å. We find other possible broad-bands in Cernis 52 at 7050 and 7133 Å which are not present in the reference stars and cannot be ascribed to known photospheric or interstellar features. The TiO γ system has bandheads at 7054, 7088 and 7125 Å but the atmospheric temperatures of both components of Cernis 52 are much higher than required for the formation of atmospheric TiO molecules and therefore cannot provide an explanation. The potential contribution to these absorptions of circumstellar or protoplanetary disc material at much cooler temperatures cannot be ruled out nor proved at present and should be further investigated.

In Fig. 2, we also overplot a synthetic spectrum of DIBs computed adopting wavelengths, widths and strengths from a comprehensive compilation in spectra of the stars HD 204827 and HD 183143 (Hobbs et al. 2008, 2009). These stars display extinctions $E(B-V)$ of 1.11 and 1.27, respectively, slightly higher than Cernis 52 and provide a valuable reference for the strength of the DIBs in our target. The assumption of a Gaussian profile was reasonable, in particular given the relatively modest resolution of our spectra, for most of the DIBs in the wavelength range of interest. For DIBs in common among these two works we adopted the equivalent widths by Hobbs et al. (2009) which are of slightly higher quality but also correspond to a higher extinction. Very few DIBs were present only in one of the two reference stellar spectra. We can identify in the spectrum of Cernis 52 absorption features coincident with previously known DIBs located at 7069.68, 7078.07, 7083–87, 7092.67 and 7106.31 Å. For these DIBs we measure equivalent widths of 7, 5, 10, 6 and ∼28 mÅ, respectively (with errors of the order of 10 per cent), which seem to be weaker in Cernis 52 than in the reference stars. We convolved the synthetic DIB spectrum to account for the resolving power of our observed spectra. Then, we scaled the DIB spectrum to provide a reasonable match to the DIBs in Cernis 52 that were located outside the region of the anthracene. In practice, we establish the scaling factor from the ratios of equivalent widths for several DIBs adjacent to the anthracene region. We find that the equivalent widths of the DIBs in our spectra compare well in strength with those in HD 204827, while a reduction of ∼30 per cent is required for the DIB spectrum provided by HD 183143. The synthetic DIB spectrum with this factor applied is plotted at the top of Fig. 2. We can see that the DIB spectrum reproduces reasonably well several absorptions in our spectra of Cernis 52, in particular the stronger DIBs at 7061, 7063, 7070 and 7120 Å. It is also clear that the DIB spectrum cannot explain the broad feature in the 7075–7105 Å range. We conclude that this feature in the spectrum of Cernis 52 cannot be of photospheric origin since it is at least 10 times broader and much stronger than photospheric lines and cannot be explained by known DIBs which are 10 times narrower and much weaker in this spectral range. To our knowledge, no such broad-band has been reported in spectra of similar stars, so we suggest that it could be associated with molecular material of circumstellar or interstellar origin.

In order to better quantify the shape and strength of a potential anthracene cation feature, we have applied corrections for both the photospheric bands and the DIBs present in the spectra. First, we removed the photospheric lines from the spectra of Cernis 52 by dividing by the synthetic photospheric spectrum of Fig. 2. Then, the resulting spectrum was divided either by the synthetic DIB spectrum of Fig. 2 or by the publicly available 'average' spectrum of stars of comparable extinction to Cernis 52 (Galazutdinov et al. 2000). These corrections were applied to the spectra of Cernis 52 obtained at both telescopes. The results obtained with each of the two DIB reference spectra are plotted in Fig. 4 where we can see that independent from the telescope (WHT or HET) and from the DIB reference spectrum used for correction (the synthetic spectrum based on the data by Hobbs et al. or the Galazutdinov et al. 'average' spectrum) we obtain as a result a broad-band remarkably close in wavelength and width to the laboratory measurements of the

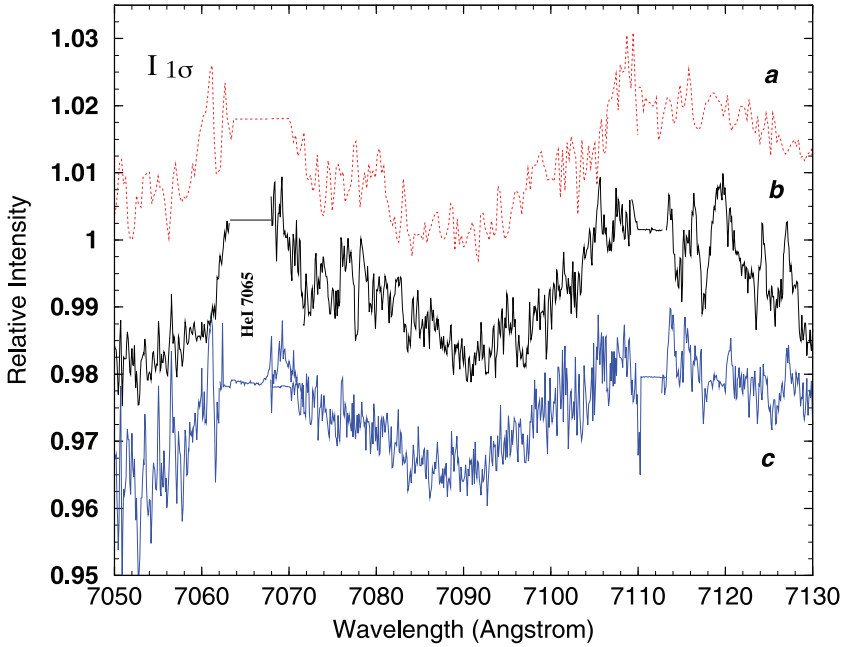

Figure 4. HET and WHT spectra of Cernis 52 corrected for the photospheric and DIB contributions. The red solid line shows the results obtained for the WHT spectrum (a) corrected using the 'average' DIB spectrum of Galazutdinov et al. (2000). The black solid line shows the HET data (b) corrected using the DIB spectrum in Fig. 2. The blue solid line shows the results for the HET data (c) corrected using the 'average' DIB spectrum. All the spectra have been normalized in the continuum to unity and shifted vertically for clarity.

strongest band of the anthracene cation. Spectra 'b' and 'c' allow us to compare the use of a 'synthetic' DIB spectrum versus a real one. The latter may describe more properly the profile of the bands but may also introduce photospheric contamination from the hot reference star. As we can see, using one approach or the other does not make a significant difference for the shape and strength of the band we are interested. Apparent minor differences in the resulting spectra can be attributed to uncertainties in the scaling and differential behaviour of DIBs with $E(B-V)$ and to the presence of small atmospheric features in the hot stars used to outline these DIBs. We caution that the 'average spectrum' used as divisor can introduce features which are difficult to trace. It is unfortunate that the blue wing of our band is affected by an He line present in hot stars (see HD 23180 spectra in Fig. 2) and certainly in the 'average reference spectrum' limiting our ability to obtain suitable corrections at a wavelength bluer than 7070 Å. This region is also closer to the edge of the order in the HET echelle data where the S/N decreases quickly.

In summary, we find in each of the three spectra plotted in Fig. 4 a broad-band with a maximum depth of about 1.5 per cent of the continuum and a central wavelength close to 7088 Å. The differences between these spectra give an idea of the uncertainties involved in the measurement of this band which is traced in the spectra of both telescopes by more than 40 resolution elements at 3σ from the continuum, leading to a very solid overall detection. In Fig. 5, we overlaid the three spectra of the previous figure. The combined WHT(a) and HET (c) spectrum can be fitted using a Lorentzian of FWHM of 40 ± 5 Å centred at 7088.8 Å. The equivalent width of the interstellar band was measured integrating the combined spectrum and resulted $W = 600 \pm 200$ mÅ where the error takes into account the differences in width and strength of the bands resulting from the various corrections applied and is largely dominated by the uncertainty in the location of the continuum.

The characteristics of the observed 7088 Å band agree reasonably well with the laboratory measurements (Sukhorukov et al. 2004) for the strongest band of the anthracene cation which give a central wavelength of 7085.7 ± 1.3 Å and an FWHM of 47 Å. The FWHM measured by Sukhorukov et al. in their direct absorption cavity ring-down spectroscopy seems to be larger than the observed value of the interstellar band, but this may well be the result of differences between the conditions of their experiment and the conditions of the cations in the interstellar medium towards Perseus. The study of the thermal dust emission at millimetre wavelengths indicates temperatures of the order of 19 K in the region causing the anomalous microwave emission (Watson et al. 2005; Tibbs et al. 2010). The laboratory band of the anthracene cation was measured when the source temperature was raised to 205°C. According to Sukhorukov et al., the absorption profile of the anthracene cation depends on the density and this is a function of the temperature. In fact at temperatures lower than 120°C the vapour pressure was too low for these authors to observe the absorption. They concluded that in their experimental setup the anthracene cations may not experience enough collisions to cool down the rotational and vibrational degrees of freedom and therefore that the widths of laboratory bands are likely to be larger than those of interstellar bands. It is interesting to note that with their experimental setup Sukhorukov et al. obtain larger widths by a factor of 1.5 for the bands of naphthalene cation than Biennier et al. (2003). The width of the interstellar band of the naphthalene cation in this line of sight is claimed by Iglesias-Groth et al. (2008) to agree well with the laboratory measurements by Biennier et al. (2003). This also supports that the interstellar band of the anthracene cation is narrower than the current laboratory band measurements.

The 7088 Å band is not only one of the strongest bands from the cation's ground state but also the sole band for which gas-phase spectroscopy has provided an accurate wavelength. Matrix

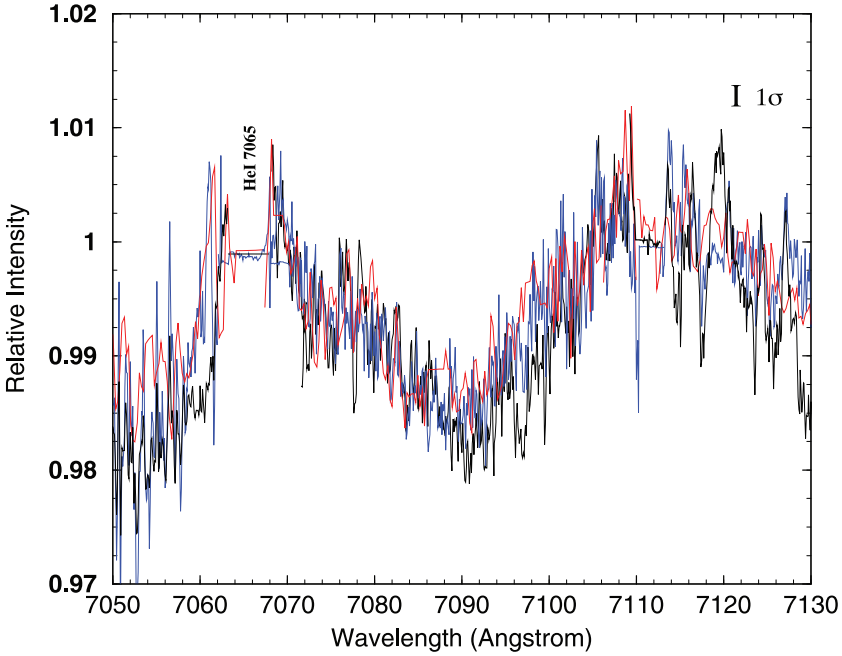

Figure 5. Overlay of the HET and WHT spectra in the previous figure.

isolation spectroscopy (MIS) (Szczepanski et al. 1993) has provided wavelengths for other bands but these measurements differ from wavelengths for free cations by amounts that are too uncertain to provide a basis for secure identification in an astronomical spectrum. For example, the MIS wavelength for the 7088 Å band is 22 Å to the red of the gas-phase measurement. The 7088 Å band is the 0-0 vibrational band of the $1^2A_u \leftarrow X^2B - 3g$ transition. The 0-0 band for $2^2A_u \leftarrow X^2B_{3g}$ is at 3520 Å from MIS with an f-value probably similar to that of 7088 Å (Niederalt, Grimme & Peyerimhoff 1995). Then, $3^2A_u \leftarrow X^2B_{3g}$ is at 3140 Å from MIS with a predicted f-value several times that of the 7088 Å band. With accurate wavelengths from gas-phase spectroscopy, it will be of interest to search for these two bands. Another sequence of transitions involves the sequence of $^2B_{1u}$ states. The initial band to 1^2B_{1u} is at 6146 Å from MIS but with an f-value a fraction of the 7088 Å band's f-value it is highly unlikely to be detectable in our spectrum even if the wavelength were known accurately. The next member of the series to 2^2B_{1u} is at 4279 Å from MIS with an f-value comparable to that for 7088 Å. The 0-0 band at 7088 Å (and the 0-0 bands of other electronic transitions) will be accompanied by a band to the lowest excited vibrational state of the 1^2B_{1u} level. For the 7088 Å band, this band will be about 190 Å to the blue according to the vibrational frequency suggested by MIS and quantum calculations (Szczepanski et al. 1993). With the f-value suggested by MIS, the band in our spectrum would have a depth of only about 0.2 per cent.

In short, attribution of the new interstellar band at 7088 Å to the anthracene cation is potentially testable when accurate laboratory wavelengths are provided for other electronic transitions. Here we will assume that the 7088.8 Å band is due to anthracene cation molecules in the cloud that causes the extinction in Cernis 52. Adopting for the oscillator strength of the transition at 7088 Å a value of $f = 0.13$ (average of those reported by Niederalt et al. 1995; Hirata, Lee & Head-Gordon 1999; Ruiterkamp et al. 2005) and using 600 mÅ as measured equivalent width of the band, we derive a column density of $N_{an^+} = 1.1 \times 10^{13}$ cm^{-2} (with an uncertainty of 40 per cent). This is very similar to the column density estimated for the naphthalene cation in the same line of sight (Iglesias-Groth et al. 2008). Assuming a ratio C/H $= 3.7 \times 10^{-4}$ and hydrogen column density per unit interstellar reddening from Bohlin, Savage & Drake (1978), we obtain $N(H) = 5.3 \times 10^{21}$ cm^{-2} and derive that ∼0.008 per cent of the total carbon in the intervening cloud could be in the form of anthracene cations.

With these low abundances, electric dipole emission of these molecules can explain only a small fraction of the anomalous microwave emission detected in the line of sight, mainly at frequencies higher than 50 GHz (Iglesias-Groth et al. 2008). It is possible that neutral PAHs are more abundant than cations and that larger PAHs exist in the cloud and contribute to the anomalous emission at frequencies in the range 10–50 GHz.

3.1 The intervening cloud

We note the existence of a reflection nebula in the line of sight of Cernis 52, clearly seen as extended optical emission in images of the Digital Sky Survey. The radial velocity of the star and of the DIBs in the spectrum agrees within 1 km s^{-1}, the uncertainty in the measurement, thus this star which is a likely member of the IC 348 cluster (González Hernández et al. 2009) could be embedded in the cloud. Observations of the K I 7698.974 Å line show only one velocity component, indicative of possibly a single cloud structure in this line of sight (see Fig. 6). Extended mid-infrared emission is also seen in archive images obtained with IRAC onboard the *Spitzer* satellite in the wavelength range 3 to 9 μm. This emission is much stronger at the 5.8 and 8.0 μm bands than at 3.6 and 4.5 μm. We attribute the high emission at long wavelengths to C–C and C–H stretching and bending modes of PAHs at 6.2 and 7.7+8.6 μm, and note that the weaker emission of the expected 3.3 μm band could be due to a significant ionization of PAHs (Iglesias-Groth et al., in preparation).

In order to provide some insight on the physical and chemical conditions and in particular on the PAH charge state distribution of the cloud in the line of sight of Cernis 52, we have measured the

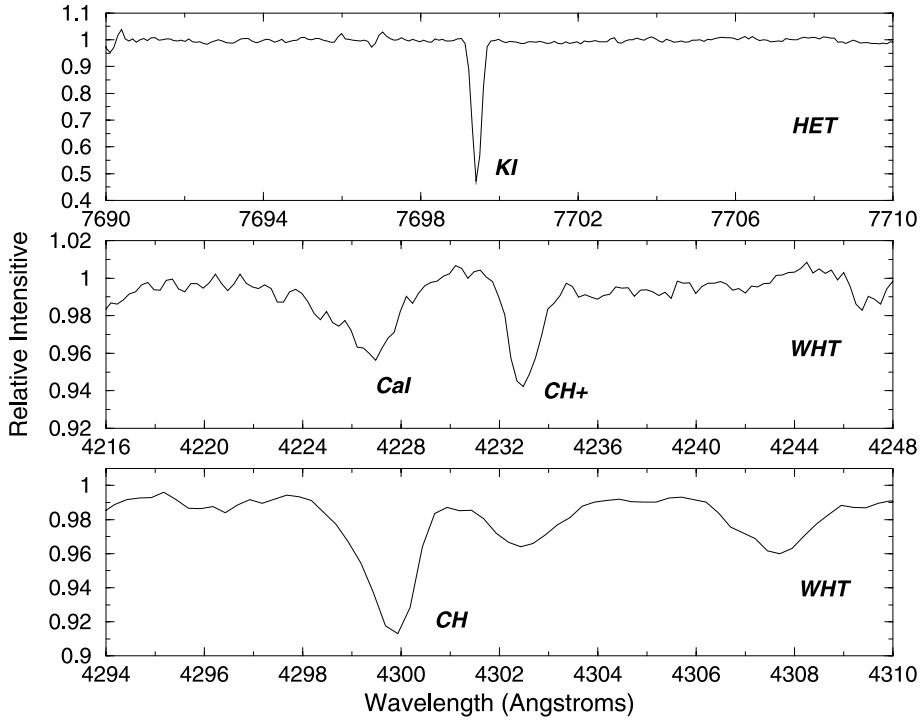

Figure 6. Top panel: the HET spectrum of Cernis 52 in the region of the K I line at 7699 Å. Middle and bottom panels: WHT spectra of Cernis 52 in the region of the A-X (0-0) bands of CH^+ and CH.

interstellar lines of CH and CH^+ at 4300.313 and 4232.548 Å available in our ISIS blue arm spectra taken in 2007 and 2008 December at the WHT. These lines have been used in the literature to study a large variety of interstellar (diffuse, translucent, dense) clouds including several with extinction similar to that of the cloud under consideration here (see e.g. de Vries & van Dishoeck 1988; Crane, Lambert & Sheffer 1995). We find the blue wing profile of the CH line slightly asymmetric possibly due to contamination by a stellar photospheric feature. We used a synthetic stellar spectrum to take into account potential contributions of photospheric lines from Cernis 52 and correct for them. The CH^+ line appears consistent with a single Gaussian profile. We measure equivalent widths of $W = 66 \pm 8$ and 70 ± 8 mÅ for the CH and CH^+ lines, respectively. These errors take into account the uncertainty in the measurement of the equivalent widths which is of the order of 5–6 mÅ and the uncertainty associated with the correction of photospheric lines which is driven by the uncertainties in the stellar parameters of Cernis 52 (González Hernández et al. 2009). We estimate uncertainties of the order of 20 per cent for the predicted equivalent widths of the photospheric lines which in both cases are minor contributors to the absorption at the wavelength of the CH features. This implies additional uncertainties of the order of 4–5 mÅ which combined quadratically with the previous error lead to the final quoted 8 mÅ error. The two sets of WHT observations taken with a time baseline of 1 year gave consistent strengths and the observed wavelengths of each set of lines agreed within 50 mÅ (4 km s^{-1}). Both CH and CH^+ lines show heliocentric velocities consistent within the uncertainties with that of the K I line observed at higher dispersion with the HET. The oscillator strength of the CH transition is $f = 0.00506$ (Brzozowski et al. 1976; Larsson & Siegbahn 1983a). In order to account for a slightly saturated line, the column density will be obtained from curves of growth with $b = 1.5$ km s^{-1}. The measured equivalent width implies then $N(\mathrm{CH}) = (2 \pm 0.2) \times 10^{14}$ cm^{-2}. Similarly, and adopting the oscillator strength of the CH^+ line from Larsson & Siegbahn (1983b), we obtain $N(CH^+) = (2 \pm 0.2) \times 10^{14}$ cm^{-2}. Both species display rather high column densities.

The average H I column density derived from the LAB map (Kalberla et al. 2005) in the direction of Cernis 52 is $N(\mathrm{H\,I}) = 1.2 \times 10^{21}$ cm^{-2}. Using the relationships between CH and H_2 in Danks, Federman & Lambert (1984) and Mattila (1986) we obtain from our N(CH) value two independent estimates of the column density for molecular hydrogen. The average value results $N(H_2) = 6.3 \times 10^{21}$ cm^{-2}. The total column density of hydrogen then is $N(\mathrm{H}) = N(\mathrm{H\,I}) + 2N(H_2) = 13.8 \times 10^{21}$ cm^{-2}. This is a factor of 2.6 larger than the value derived from the excess colour $E(B - V)$ of Cernis 52. Possibly indicating that the A_V and $E(B - V)$ relation is steepened in this cloud. It seems that we deal with a cloud that causes a total visual extinction significantly higher than in typical diffuse interstellar clouds and comparable or even higher than translucent molecular clouds (see e.g. van Dishoeck & Black 1989). Models for clouds of similar characteristics can be found, for example, in Ruiterkamp et al. (2005) who include a detailed treatment of the PAH charge state distribution. It is apparent from their fig. 3 that PAHs with a low number of carbon atoms are mostly expected in a neutral stage, in particular anthracene and naphthalene cations charge fractions are expected of the order of 10 per cent while the neutral species could be as abundant as 65 per cent and anions would provide the remaining fraction. Changes in the hydrogen density (in the recombination rate) or in the intensity of the ultraviolet (UV) radiation field (in the ionization rate) do not drastically affect this result for this type of cloud.

The derived column densities of CH and CH^+ in the cloud towards Cernis 52 are significantly higher than in any other CH surveys of diffuse interstellar clouds, including examples of clouds of higher extinction. The high abundance of these species and also of molecular hydrogen is an indication of a potentially rich chemistry that

may convert atoms into organic molecules (see e.g. Millar 2004 for the reaction networks involved) at the observed column densities towards Cernis 52. In less rich clouds previously surveyed in the literature the column density of anthracene and naphthalene may be considerably lower and their bands weaker. This could explain why the anthracene and naphthalene cation bands discussed here and in Iglesias-Groth et al. (2008) have escaped detection in other lines of sight. Another reason for the lack of previous detections of the anthracene cation is that DIB surveys are frequently conducted using high-dispersion echelle spectrographs which have difficulties to detect weak, very broad features due to continuum correction.

We have examined the behaviour of the major DIBs in the various spectra of Cernis 52 available to us (including those obtained by Iglesias-Groth et al. 2008 at the 3.6-m Telescopio Nazionale Galileo and the 2.7-m at the McDonald Observatory) with the aim to identify any possible anomalous behaviour which could be related to the dust properties of the cloud. Here, we present results for the two major diffuse bands at 5780 and 5797 Å. These two diffuse bands discovered by Heger (1922) show strength ratios that vary with the shape of the extinction curve (Krełowski et al. 1987). High molecular abundances – as for CH in the line of sight of Cernis 52 – appear in interstellar clouds characterized by a broad UV extinction bump (2175 Å), steep far-UV extinction and low 5780/5797 diffuse band intensity ratio. Such clouds are called 'zeta'-type clouds (Krełowski & Sneden 1995) and present strong molecular features in their spectra. Examples of these clouds are found towards stars like ζ Per and HD 23180 in Perseus where the 5780/5797 ratios (equivalent widths of 5780 to 5797) range between 1 and 2 (Krełowski, Megier & Strobel 1996). Such values are much lower than those found by these authors in the so-called 'sigma' clouds which present strikingly different extinction curves (see for a discussion Krełowski, Sneden & Hiltgen 1995). In Fig. 7, we plot our McDonald spectra of Cernis 52 in the spectral range of these DIBs in comparison with HD 23180. It is remarkable the similar strength of the 5780 DIB in both stars while the 5797 DIB is clearly stronger in Cernis 52. This leads to a smaller 5780/5797 ratio than in HD 23180 and fully supports the classification of the intervening cloud towards Cernis 52 as of 'zeta' type. To our knowledge the UV extinction curve in this line of sight is unknown but based in the behaviour of the 5780/5797 DIBs we may expect a steep far-UV extinction. It is well established that some diffuse bands like the 5797 Å correlate positively with the overall slope of the extinction curve while others like the 5780 Å show negative correlation (Megier, Krełowski & Weselak 2005). A positive correlation with the overall slope probably indicates an anticorrelation with the UV irradiation and the carrier of the 5797 Å band may benefit from shielding. If this is the case shielding is more effective in the Cernis 52 cloud than in the 'zeta' cloud towards the star HD 23180 (also in Perseus but in a region without significant anomalous microwave emission). The band at 5780 Å, known to be more resistant to strong UV fields than the 5797 DIB, shows similar strength in both clouds. The DIB at 5850 Å is known to closely follow the behaviour of the 5797 DIB and correlates with the overall slope of extinction (Megier et al. 2005). We find that the strength of this DIB in Cernis 52 is also a factor of 2 higher than in HD 23180. The extinction in the UV reduces the flux of the UV radiation that is believed to ionize or destroy the carriers of these bands.

We have scrutinized our spectra to search for bands of other PAHs with reliable gas-phase measurements (see Salama 2008) and confirm in our new data the naphthalene band at 6707 Å previously found by Iglesias-Groth et al. (2008). At various wavelengths we find marginal evidence for other broad-bands that may correspond to PAH cations, and for relatively narrow absorptions that could be associated with carbon chains and carbon rings but confirmation may require higher quality measurements. The upper limits we can impose on the column densities of these other PAHs do not bring at this stage sufficient information to establish the reaction networks in the cloud. A comprehensive analysis of the DIBs in the line of sight of Cernis 52 may also provide additional information on the UV radiation field in the intervening cloud but this is beyond the scope of this paper and will be the subject of a dedicated more comprehensive work.

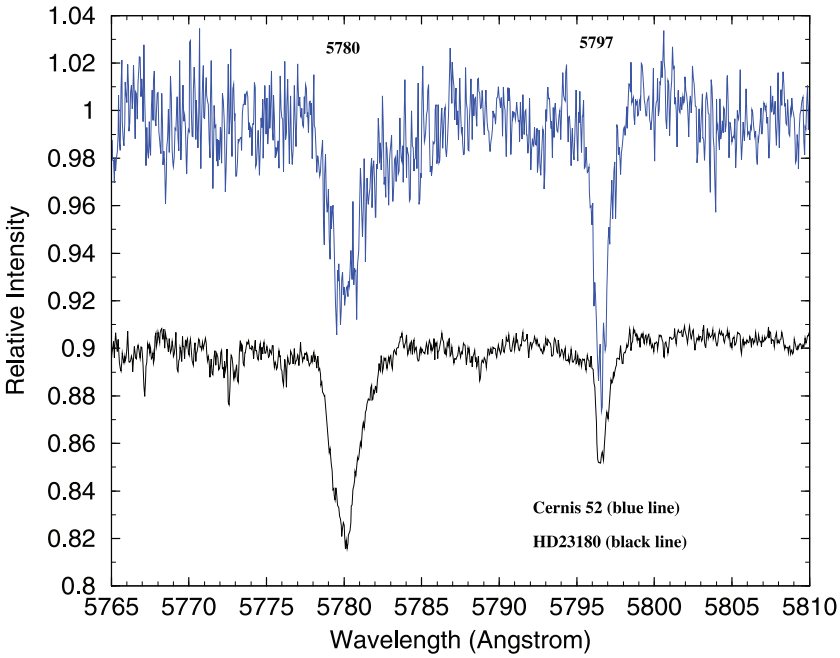

Figure 7. Spectra of Cernis 52 (blue line) and HD 23180 (black line) in the region of the DIBs at 5780 and 5797 Å.

4 CONCLUSIONS

We report the discovery of a new broad-band at 7088.8 ± 2 Å in the spectrum of Cernis 52 with wavelength and width consistent with gas-phase measurements of the strongest band of the anthracene cation. This is the only band of the anthracene cation with a wavelength measured from gas-phase spectroscopy. We measure an equivalent width of $W = 600 \pm 200$ mÅ. Assigning the observed band to this cation, we infer a column density of $N_{\rm an^+} = 1.1(\pm0.4) \times 10^{13}\,{\rm cm}^{-2}$. This value is very close to previous estimates for the column density of naphthalene cations in the same line of sight $N_{\rm naph^+} = 1.0(\pm0.6) \times 10^{13}\,{\rm cm}^{-2}$ (Iglesias-Groth et al. 2008). It appears that the intervening cloud contains the same amount of cations of anthracene and naphthalene. We also detect bands of CH and CH^+ at 4300.313 and 4232.548 Å from which we obtain column densities for these species of $2(\pm0.2) \times 10^{14}$ cm^{-2} and infer a rather high column density for molecular hydrogen $N(H_2) = 6.3 \times 10^{21}$ cm^{-2}. Observations of the K I line are consistent with the existence of a single cloud in the line of sight. Measurements of the major DIBs at 5780 and 5797 Å clearly indicate that the intervening cloud is of 'zeta' type, probably with a steep far-UV extinction.

The cloud towards Cernis 52 is likely to be responsible for the anomalous microwave emission reported in this line of sight. The presence of PAHs in a region of strong anomalous microwave emission adds support to the hypothesis that electric dipole radiation by these types of molecules is responsible for the excess emission detected in the 10–50 GHz range. The abundance of PAHs was taken as a free parameter in models attempting to explain this anomalous microwave emission (Draine & Lazarian 1998). The abundances derived for naphthalene and anthracene cations provide additional constraints for these models.

Laboratory experiments at low temperatures (15 K) have shown that UV radiation on a mixture of naphthalene, ammonia and H_2O ice leads to the formation of a large variety of amino acids (Chen et al. 2008). In the line of sight of Cernis 52, there is evidence for ammonia (Rosolowsky et al. 2008) with a column density quite similar to what we find for the most simple PAHs. The likely presence of H_2O ices combined with the UV radiation from Cernis 52 could make this region in Perseus a potential factory for amino acids. The detection of specific PAHs in the molecular cloud towards Cernis 52 may help to identify a possible path for biogenic compounds from the chemistry of clouds (where new stars form) to the pre-biotic molecules detected in protoplanetary discs. Further studies in this remarkable region have the potential to reveal a very rich interstellar pre-biotic chemistry.

ACKNOWLEDGMENTS

We acknowledge support front grant AYA-2007-64748 from the Spanish Ministry of Science and Innovation and also thank the McDonald Observatory's Hobby–Eberly Telescope time allocation committee for their exceptional support. DLL thanks the Robert A. Welch Foundation of Houston for support via grant F-634. JIGH thanks financial support from the Spanish Ministry project MICINN AYA2008-00695. DAGH acknowledges support from the Spanish Ministry of Science and Innovation (MICINN) under the 2008 Juan de la Cierva Programme.

REFERENCES

Allamandola L. J., Tielens G. G. M., Barker J. R., 1989, ApJS, 71, 733, 1989
Allende Prieto C., Barklem P. S., Lambert D. L., Cunha K., 2004, A&A, 420, 183
Biennier L. et al., 2003, J. Chem. Phys., 118, 7863
Bohlin R. C., Savage B. D., Drake J. F., 1978, ApJ, 224, 132
Brzozowski J., Bunker P., Elander N., Erman P., 1976, ApJ, 207, 414
Casassus S., Cabrera G. F., Förster F., Pearson T. J., Readhead A. C. S., Dickinson C., 2006, ApJ, 639, 951
Cernis K., 1993, Balt. Astron., 2, 214
Chen Y.-J., Nuevo M., Yih T.-S., Ip W.-H., Fung H.-S., Cheng C.-Y., Tsai H.-R., Wu C.-Y. R., 2008, MNRAS, 84, 605
Crane P., Lambert D. L., Sheffer Y., 1995, ApJS, 99, 107
Danks A. C., Federman S. R., Lambert D. L., 1984, A&A, 130, 62
de Oliveira-Costa A. et al., 1999, ApJ, 527, L9
de Oliveira-Costa A. et al., 2002, ApJ, 567, 363
de Vries C. P., van Dishoeck E. F., 1988, A&A, 203, L23
Draine B. T., Lazarian A., 1998, ApJ, 494, L19
Galazutdinov G. A., Musaev F. A., Krełowski J., Walker G. A. H., 2000, PASP, 112, 648
González Hernández J. I., Iglesias-Groth S., Rebolo R., García-Hernández D. A., Manchado A., Lambert D. L., 2009, ApJ, 706, 866
Heger M. L., 1922, Lick Obs. Bull., 10, 146
Hildebrandt S. R., Rebolo R., Rubio-Martín J. A., Watson R. A., Gutiérrez C. M., Hoyland R. J., Battistelli E. S., 2007, MNRAS, 382, 594
Hirata S., Lee T. L., Head-Gordon M., 1999, J. Chem. Phys., 111, 8904
Hobbs L. M. et al., 2008, ApJ, 680, 1256
Hobbs L. M. et al., 2009, ApJ, 705, 32
Iglesias-Groth S., 2005, ApJ, 632, L25
Iglesias-Groth S., 2006, MNRAS, 368, 1925
Iglesias-Groth S., Manchado A., García-Hernández D. A., González Hernández J. I., Lambert D., 2008, ApJ, 685, L55
Kalberla P. M. W., Burton W. B., Hartmann D., Arnal E. M., Bajaja E., Morras R., Pöppel W. G. L., 2005, A&A, 440, 775
Krełowski J., Sneden C., 1995, in Tielens A. G. G. M., Snow T. P., eds, Proc. IAU Colloq. 137, The Diffuse Interstellar Bands. Kluwer, Dordrecht, p. 13
Krełowski J., Walker G. A. H., Grieve G. R., Hill G. M., 1987, ApJ, 316, 449
Krełowski J., Sneden C., Hiltgen D., 1995, Planet. Space Sci., 43, 1195
Krełowski J., Megier A., Strobel A., 1996, A&A, 308, 908
Kogut A., Banday A. J., Bennett C. L., Gorski K. M., Hinshaw G., Reach W. T., 1996, ApJ, 460, 1
Larsson M., Siegbahn P. E. M., 1983a, Chem. Phys., 79, 2270
Larsson M., Siegbahn P. E. M., 1983b, Chem Phys., 76, 175
Leitch E. M. et al., 1997, ApJ, 486, L23
Mattila K., 1986, A&A, 160, 157
Megier A., Krełowski J., Weselak T., 2005, MNRAS, 358, 563
Millar T. J., 2004, in Ehrenfreund P. et al., eds, Organic Molecules in the Interstellar Medium in Astrobiology: Future Perspectives, Kluwer, Dordrecht, p. 17
Niederalt C., Grimme S., Peyerimhoff S. D., 1995, Chem. Phys. Lett., 245, 455
Puget J. L., Léger A., 1989, ARA&A, 27, 161
Rosolowsky E. W., Pineda J. E., Foster J. B., Borkin M. A., Kauffmann J., Caselli P., Myers P. C., Goodman A. A., 2008, ApJS, 175, 509
Ruiterkamp R., Cox N. L. J., Spaans M., Kaper L., Foing B. H., Salama F., Ehrenfreund P., 2005, A&A, 432, 515
Salama F., 2008, in Kwok S., Sandford S., eds, Proc. IAU Symp. Vol. 251, Organic Matter in Space. Cambridge Univ. Press, Cambridge, p. 357
Sukhorukov O., Staicu A., Diegel E., Rouillé G., Henning Th., Huisken F., 2004, Chem. Phys. Lett., 386, 259
Szczepanski J., Vala M., Talbi D., Parisel O., Ellinger Y., 1993, J. Chem. Phys., 98, 4494
Tibbs C. et al., 2010, MNRAS, 402, 1969
van Dishoeck E. F., Black J. H., 1989, ApJ, 340, 273
Watson R. A. et al., 2005, ApJ, 624, L89

This paper has been typeset from a TEX/LATEX file prepared by the author.